Acta Oceanol. Sin., 2024, Vol. 43, No. 2, P. 43–57
https://doi.org/10.1007/s13131-023-2264-9
http://www.aosocean.com
E-mail: ocean2@hyxb.org.cn

Coral records of Mid-Holocene sea-level highstands and climate responses in the northern South China Sea

Yuanfu Yue[1, 2*], Lichao Tang[1, 2], Kefu Yu[1, 2*], Rongyong Huang[1, 2]

[1] School of Marine Sciences, Coral Reef Research Center of China, Guangxi University, Nanning 530004, China

[2] Guangxi Laboratory on the Study of Coral Reefs in the South China Sea, Nanning 530004, China

Received 14 July 2023; accepted 6 September 2023

Abstract

High-resolution sea-level data and high-precision dating of corals in the northern South China Sea (SCS) during the Holocene provide a reference and historical background for current and future sea-level changes and a basis for scientific assessment of the evolutionary trend of coral reefs in the SCS. Although sporadic studies have been performed around Hainan Island in the northern SCS, the reconstructed sea level presents different values or is controversial because the indicative meaning of the sea-level indicators were neither quantified nor uniform criteria. Here, we determined the quantitative relationship between modern living coral and sea level by measuring the top surfaces of 27 live *Porites* corals from the inner reef flat along the east coast of Hainan Island and assessed the accuracy of results obtained using coral as sea-level indicators. Additionally, three *in situ* fossil *Porites* corals were analyzed based on elevation measurements, digital X-ray radiography, and U-Th dating. The survey results showed that the indicative meanings for the modern live *Porites* corals is (146.09 ± 8.35) cm below the mean tide level (MTL). It suggested that their upward growth limit is constrained by the sea level, and the lowest low water is the highest level of survival for the modern live *Porites* corals. Based on the newly defined indicative meanings, 6 new sea-level index points (SLIPs) were obtained and 19 published SLIPs were recalculated. Those SLIPs indicated a relative sea level fluctuation between (227.7 ± 9.8) cm to (154.88 ± 9.8) cm MTL between (5 393 ± 25) cal a BP and (3 390 ± 12) cal a BP, providing evidences of the Mid-Holocene sea-level highstand in the northern SCS. Besides that, our analysis demonstrated that different sea-level histories may be produced based on different indicative meanings or criteria. The dataset of 276 coral U-Th ages indicates that coral reef development in the northern SCS comprised the initial development, boom growth, decline, and flourishing development again. A comparison with regional records indicated that synergistic effects of climatic and environmental factors were involved in the development of coral reefs in the northern SCS. Thus, the cessation of coral reef development during the Holocene in the northern SCS was probably associated with the dry and cold climate in South China, as reflected in the synchronous weakening of the ENSO and East Asian summer monsoon induced by the reduction of the 65°N summer insolation, which forced the migration of the Intertropical Convergence Zone.

Key words: northern South China Sea, Middle Holocene, sea-level highstand, *Porites* corals, climate response

Citation: Yue Yuanfu, Tang Lichao, Yu Kefu, Huang Rongyong. 2024. Coral records of Mid-Holocene sea-level highstands and climate responses in the northern South China Sea. Acta Oceanologica Sinica, 43(2): 43–57, doi: 10.1007/s13131-023-2264-9

1 Introduction

The global average sea level is showing a continuous upward trend because of global warming (Climate Change Center of the China Meteorological Administration, 2022). Sea-level rise and associated disasters are major threats to human survival, social and economic development, and the environment in low-lying coastal areas worldwide; consequently, it has become an important concern in international global change research (IPCC, 2021). For example, beach submergence (Zhang et al., 2011; Webster et al., 2016), accelerated coastal erosion (Zhang et al., 2004; Anderson et al., 2015), more extreme flood events in coastal areas (Kriebel et al., 2015; Vitousek et al., 2017; Taherkhani et al., 2020), and increased damage from destructive storms (Emanuel, 2005; Webster et al., 2005; Landsea, 2005; Klotzbach, 2006; Knutson et al., 2010; Cheng et al., 2019; Yue et al., 2019) have occurred. Therefore, sea-level rise has attracted widespread attention from the international community and governments of coastal countries. Although this crisis has been identified, a complete understanding of the history, patterns, and driving mechanisms of past sea-level changes is currently lacking. Therefore, definitive conclusions cannot be made about whether future sea-level rises will accelerate and reach high sea levels as in the Middle Holocene, which has seriously affected the accuracy of our predictions of future sea-level changes. More importantly, past climate change is the background for contemporary and future climate and environmental changes. To address global change, historical sea-level conditions and change patterns must be better understood, especially the changes in the Holocene as the changes that occurred in this period is closely associated with modern environmental changes. For instance, robust evidence has shown that the Mid-

Foundation item: The National Natural Science Foundation of China under contract Nos 42366002 and 41702182; the National Key R&D Program of China under contract No. 2017YFA0603300; the Guangxi Scientific Projects under contract No. 2018GXNSFAA 281293.

*Corresponding author, E-mail: yuanfu.yue@gxu.edu.cn; kefuyu@scsio.ac.cn

Holocene was a high-temperature period with a climate similar to the modern climate but much warmer (Gagan et al., 1998; Yu et al., 2005; Wei et al., 2007), and Mid- to Late-Holocene sea-level records from low-latitude regions serve as an important baseline of natural past sea-level change and global ice volume prior to the Anthropocene (Hallmann et al., 2018; Yue and Tang, 2023). Therefore, an in-depth understanding of past sea-level change processes and trends is required to further explore their relationship with climate change. This in turn will facilitate better prediction of future sea-level change scenarios and evaluation of their impacts, and is essential for human survival and social development.

In terms of historical sea-level changes, sea-level indicators that reflect sea-level changes must be identified (Wang, 1989; Nie, 1996) and the elevation and age of the indicators must be accurately measured to understand the historical process of sea level changes (Engelhart et al., 2011). In recent decades, with the improvement of research techniques and experimental devices, various sea-level indicators (such as foraminifera, diatoms, coral reefs, beach rocks, salt marshes, peat), reconstruction methods, and even modern observation records (~100 years, as far back as 1925 CE in Macao) have been used to broadly and intensively study historical sea-level changes in the South China Sea (SCS) along the coast, and large amounts of Holocene sea-level data have been published (Zhao and Yu, 2002; Yu et al., 2002, 2009; Zong, 2004; Huang et al., 2007; Shi et al., 2008; Yao et al., 2013; Xiong et al., 2018; Liu et al., 2020; Ma et al., 2021; Yan et al., 2021; Tao et al., 2022; Yue and Tang, 2023; Tang and Yue, 2023). For instance, Zong (2004) and Xiong et al. (2018) reconstructed the Holocene sea-level history for the lower latitudes of the Chinese coast based on ^{14}C data and suggested that the Mid-Holocene sea level was similar to the modern mean sea-level (MSL) or changed little during the past 7 000 years. Conversely, both U-Th and ^{14}C ages for *Porites* corals and *Porites* microatolls from records collected from the coastal Lei-Qiong area (an abbreviation for the Leizhou Peninsula and Hainan Island) in the northern SCS indicated a higher sea level above the modern MSL during the Mid-Holocene (Zhao and Yu, 2002; Huang et al., 2007; Shi et al., 2008; Yu et al., 2009; Yao et al., 2013).

However, observational records are too short and the reconstructed sea levels in the northern SCS differ or are controversial due to the selection of different sea-level indicators and the use of different methods (Yao et al., 2013; Yue and Tang, 2023). Moreover, whether the exposed dead *Porites* corals are the product of high sea level in the Mid-Holocene or the result of tectonic uplift has not been determined (Yao et al., 2013). Consequently, simply providing a historical reference for the trend of sea-level changes in the context of modern climate change is not a reliable method and accurate prediction of future sea-level changes is difficult. Therefore, the historical sea-level in the northern SCS must be reconstructed by selecting more precise sea-level indicators and using more accurate dating methods to clarify the existing differences.

Furthermore, the northern coast of the SCS is one of the key areas of the transition from the SCS to land and is an area sensitive to global change, as represented by Hainan Island, a far-field island located in low-latitude regions far away from the former and present ice sheet margins. The coast of this area is affected by sea-level change and has developed a larger area of fringing reef in the Holocene (Yu, 2000; Zhao and Yu, 2002), which likely represents the northern margin and coral reef distribution belt of the SCS. Of particular significance are the microatolls (commonly *Porites* microatolls), which are intertidal individual colonies with relatively flat and dead upper surfaces surrounded by an annular rim of living coral (Woodroffe and McLean, 1990; Yu et al., 2009; Smithers, 2011; Meltzner and Woodroffe, 2015). Their upward growth limit is constrained by the sea level through prolonged subaerial exposure at the lowest spring tide/lowest low water (LLW), although polyps on the colony sides remain alive and continue to grow laterally, thereby adopting a microatoll form (Woodroffe and McLean, 1990; Yu et al., 2009; Smithers, 2011; Meltzner and Woodroffe, 2015). Typically, most microatolls develop from massive *in situ* corals in shallow waters, and *Porites* microatolls are particularly common, although intertidal *Goniastrea* and *Platygyra* colonies also form microatolls on many reefs (Smithers, 2011). In flat reef settings, the upper surfaces were limited by past sea levels (Woodroffe and McLean, 1990) and thus have the potential to serve as reliable sea-level indicators (Scoffin and Stoddart, 1978; Stoddart and Scoffin, 1979; Woodroffe and McLean, 1990; Smithers, 2011; Meltzner and Woodroffe, 2015). Additionally, the U-Th dating method has been successfully developed for dating corals, enabling high-precision and accurate dating of coral reefs in this area (Zhao and Yu, 2002; Yu et al., 2009; Yan et al., 2019). Under these conditions, combining fossil corals with appropriate dating methods can provide an effective tool for accurately reconstructing the timing and trajectory of local sea-level fluctuations and revealing how Holocene climate change affected coral reef growth.

Previous studies have either focused on the history of reef growth (Zhao and Yu, 2002; Huang et al., 2007; Yan et al., 2019; Chen et al., 2021) or the reconstruction of sea-level changes during certain periods of the Holocene in the northern SCS (Shi et al., 2008; Yu et al., 2009; Yan et al., 2021). Unfortunately, these studies only collected small amounts of data, did not include tectonic corrections, and rarely included *Porites* (microatolls) elevations that were directly established by surveys to a precise datum. Therefore, a comprehensive understanding of Holocene sea-level changes and coral reef development and responses to regional environment and climate is currently lacking.

To provide a comprehensive understanding of historical sea-level changes and a necessary scientific basis for the prediction of future sea-level changes, this study determines the quantitative relationship between modern living coral and sea level by measuring the upper surfaces of 27 modern live *Porites* corals along the east coast of Hainan Island, and produces new high-quality sea-level index points (SLIPs). Based on this, we focus on reconstructing a detailed Mid-Holocene sea-level history based on elevation measurements and U-Th ages for three *in situ* exposed fossil *Porites* corals and 19 recalculated SLIPs. Additionally, our new record and an additional 270 available published coral U-Th ages from the coral reef areas along the northern coast of the SCS were further analysed and compiled. These findings will provide critical insights into major episodes of coral reef development and their relationship with climate change and a context for understanding modern ecological states.

2 Regional setting

The SCS is a semi-enclosed marginal sea located along southern mainland China and adjacent to the western Pacific Ocean (Fig. 1), and is connected to the Indo–Pacific Warm Pool. The Asian Monsoon system is composed of the South Asian (or Indian), western North Pacific, and East Asian subsystems (Wang et al., 2017). The SCS is under the effect of the East Asian Monsoon system, which is influenced by the East Asian Summer Monsoon (EASM) in summer (May–September) and East Asian Winter Monsoon (EAWM) in winter (October–April). As shown in

Fig. 1a, in winter, the EAWM creates an anticlockwise pattern of circulation, with the wind pushing cooler coastal waters down though the Taiwan Strait, where they circulate west and southwards along the coast of China (Yu and Liu, 1993; Morton and Blackmore, 2001). As shown in Fig. 1b, in summer, under the influence of the EASM, the current flow in the SCS is reversed and water enters from the Java Sea via the Karimata Straits, travels to the central area, and exits through the Taiwan Strait (Yu and Liu, 1993; Morton and Blackmore, 2001). The coastal current is controlled by monsoon dynamics, and northeast and southwest winds alternate periodically in winter and summer. Additionally, this area suffers frequent and intense storms (Yue et al., 2019).

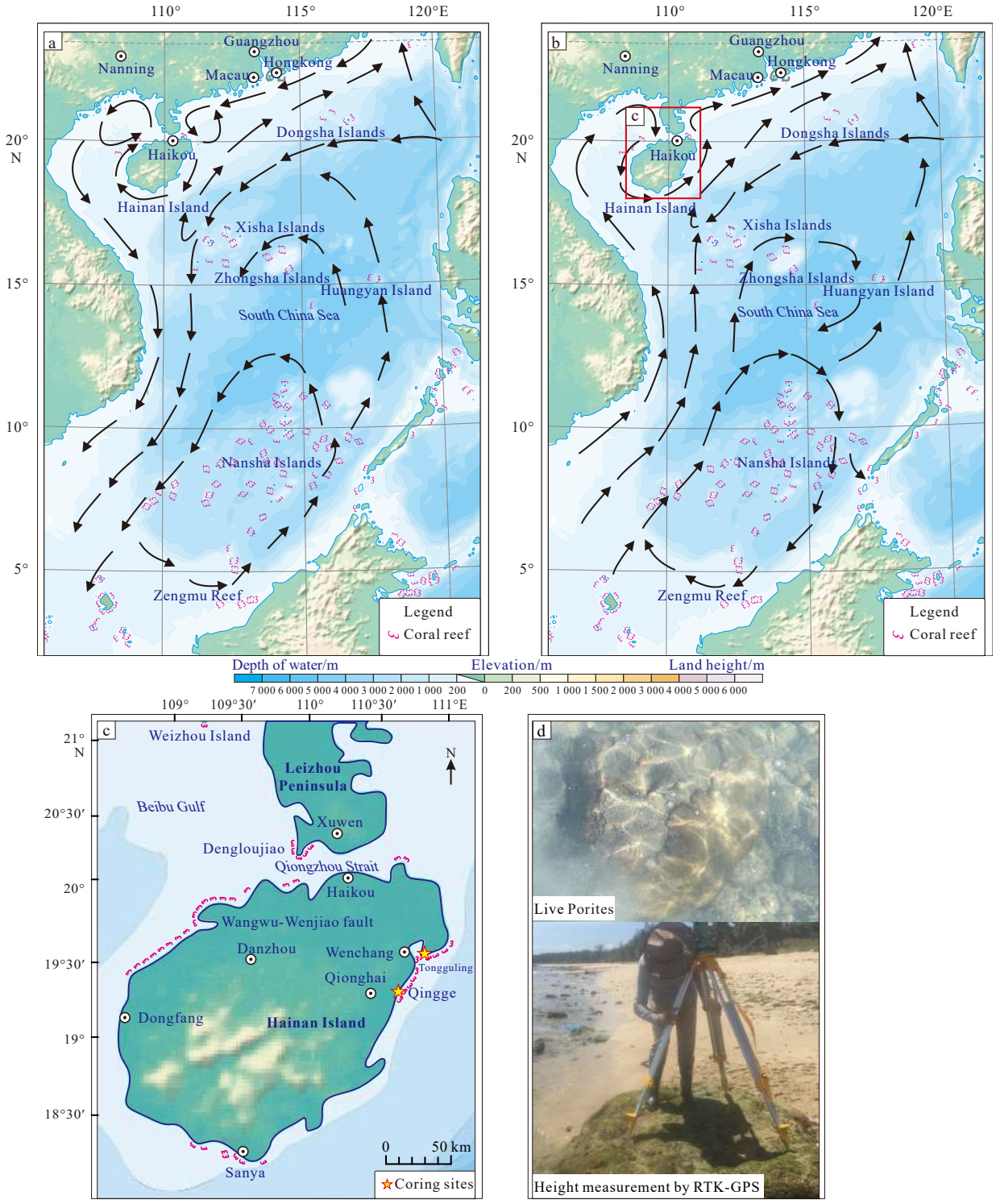

Fig. 1. A geographic map of South China Sea, showing the location of Hainan Island. a. Surface-ocean circulation patterns in the South China Sea during the East Asian Summer Monsoon (EASM) and b. the East Asian Winter Monsoon (EAWM)), modified after Yu and Liu (1993) and Morton and Blackmore (2001). c. Coral reefs are distributed along the coast of Lei-Qiong. d. The elevation survey and sampling during the field investigation from Wenchang southward to Qionghai along the east coastal Hainan Island in July 2020.

The northern SCS, including the Lei-Qiong area, Weizhou Island of Beibu Gulf, and Xisha Islands, is adjacent to the north edge of the Intertropical Convergence Zone (ITCZ) and represents a key pathway of the EASM and a major moisture source for EASM precipitation in summer. As shown in Fig. 1c, the coast of the Lei-Qiong area is located at the northern fringe of the tropics and occupies the main part of the northern coast of the SCS. Hainan Island is situated at the southern tip of China (Fig. 1c). Fringing reefs with a total length of approximately 200 km along Hainan Island are discontinuously distributed along the east and west coast of Hainan Island (Lu et al., 1984), including along the Wenchang, Qionghai, Danzhou, Dongfang, and Sanya areas (Fig. 1c). However, the coral reefs in this area and even worldwide have experienced severe bleaching due to increased human activities and global warming, with recent increases in frequency and severity being observed (Yu et al., 2012; Hughes et al., 2017; Barkley et al., 2018; Claar et al., 2018; Dalton et al., 2020; Romero-Torres et al., 2020).

Hainan Island has a tropical monsoon climate. Instrumental data from the Qionghai Meteorological Station shows that the mean annual (air) temperature is 24.62℃ for the period 1980–2010 CE (Fig. S1, Table S1). The instrumentally obtained sea surface temperature (SST) from four adjacent ocean stations in the Lei-Qiong sea area indicated that the mean annual SST is (24.85 ± 0.39)℃ (Yu, 2000), which is within the range suitable for coral growth and coral reef development on the coast (Guan et al., 2015). Notably, the SST in winter is lower than 20℃ and seasonal changes in SST moderate the growth of the coral reefs (Lu et al., 1984; Yu, 2000).

3 Materials and methods

To uncover details of sea-level change in the northern SCS during the Mid-Holocene, it is necessary to establish the indicative meaning of live *Porites* corals for SLIPs. Firstly, the top surface elevation of 27 modern live *Porites* corals obtained from the inner reef flat of the east coast of Hainan Island were measured using real-time kinematic (RTK) global positioning system (GPS) during our field surveys at the lowest low water (LLW) in July 2020 CE (Figs 1c, d). This survey was expected to help improve our ability to accurately define the indicative meaning and potential uncertainty range of modern live *Porites* corals. Secondly, the top surface elevation of three *in situ* fossil *Porites* corals which are now exposed above the tide on the inner reef flat were also measured, and then sampled. Those *Porites* corals were further polished into 7-mm thick coral plates, and then selected for X-ray radiography analyses. After performing digital X-ray radiography analyses, six subsamples were selected for U-Th dating, and six new U-Th ages and SLIPs were obtained.

Additionally, a total of 276 published U-Th ages of corals from the coral reef areas along northern coast of the SCS were collected and recalculated, including 19 region's previously published SLIPs. We recalibrated the 19 SLIPs from *Porites* corals using the newly defined indicative meanings, which were also subjected to tectonic correction, error analysis, and reliability assessment. The distribution of episodes of coral growth in the northern SCS during the Holocene was determined based on the order of U-Th ages and two standard deviations (~50-year intervals) of the age determination errors (± 2σ). Details on the data processing and methods are provided in the Supplementary Material.

4 Results

4.1 *Biological geomorphology*

During our field investigations in July 2020, several biological-geomorphological zones along the coast of Tongguling (Wenchang) southward to Qingge (Qionghai) (Fig. 1c) were generally recognized from the fringing reef. For instance, from the sea to the land, we observed reef fronts with living coral clusters, an outer reef flat coral zone that was dominated by massive *Porites* and microatolls, a middle reef flat massive coral mixed zone, an inner reef-flat branch-coral/sand zone, and sandy beach (Fig. 2).

The slope of the reef front is dominated by several types of live corals. The outer reef flat contains many *in situ* massive dead *Porites*. A few live *Porites*, *Porites* microatolls, and *Platygyra* were observed in the low-lying areas, in addition to several other hermatypic corals, such as *Montipora solanderi*, *Acropora austera*, *Facia speciose*, *Pocillopora*, and *Fungia fungites*. The middle reef flat is wide and relatively flat, with accumulations of coral debris, mainly dominated by *Acropora* spp. Generally, live corals were not observed, while numerous *in situ* dead corals were identified.

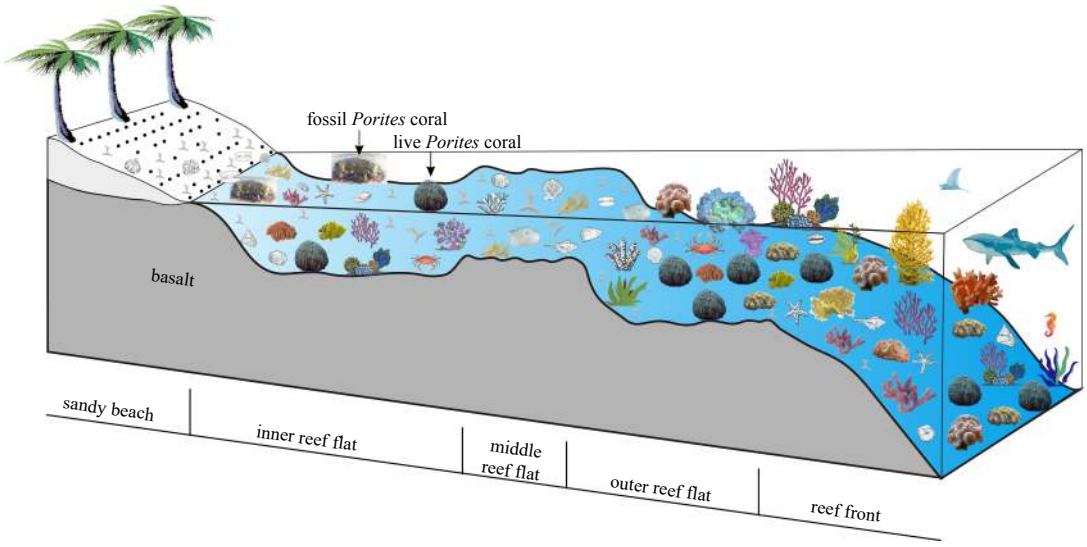

Fig. 2. Cross-section sketches showing distribution of biological-geomorphological zones of typical fringing coral reefs based on our field investigation in July 2020 on the eastern coast of Hainan in the northern SCS.

The upper surface of the inner reef flat, characterized by the presence of numerous dead *Porites* and *Porites* microatolls. The sandy beach is distributed with scores of granite outcrops and a small number of coral debris. The sand embankment is approximately 3 m higher than the average sea level. Many coconut trees and some villages and ponds are located behind the sand embankment.

4.2 *Indicative meanings for the modern live Porites corals*

Porites corals represent sea-level indicators that have a quantifiable vertical relationship to a reference tidal level, meaning that they can serve as indicators; thus, these corals were examined and quantified in this study. According to our survey, the surface elevations the modern live *Porites* corals derived from Tongguling along the coast of Wenchang, Hainan Island were within −51.60 cm to −34.94 cm with an average elevation of −43.09 cm that varied within ± 8.33 cm (corresponding to a maximum range of 16.66 cm). Namely, results show that the indicative meanings for the modern live *Porites* corals is 146.09 cm below the mean tide level (MTL), or 15.09 cm below the LLW (Fig. 3, Table S2). This finding suggested that their upward growth limit is constrained by the sea level, and the LLW is the highest level of survival for the modern live *Porites* corals. Additionally, our investigations discovered that the top surface of each *Porites* coral from this area has a significantly narrow growth range and is almost uniformly horizontal. Accordingly, a relatively consistent relationship between *Porites* corals and tidal levels emerges.

4.3 *U-Th isotopic data and age*

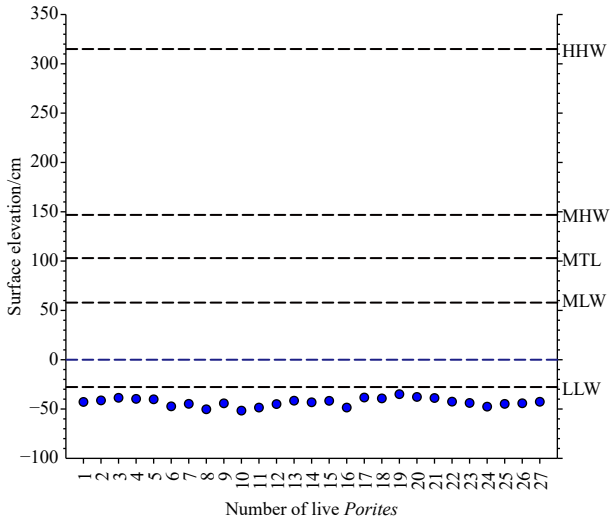

Fig. 3. Precise height measurement results of the top surface elevation of the 27 live *Porites* corals from Tongguling along the coast of Wenchang, Hainan Island. It showed that the upper surface elevations of those live *Porites* corals were 146.09 cm below the MTL on average. The depth range of live *Porites* corals heights is relative to 1985 National Elevation Benchmarks and the predicted tidal levels at Qinlan Port tide gauge. The mean tide level (MTL) lies 103 cm above 1985 National Elevation Benchmarks, the mean low water (MLW) is 58 cm, the mean high water (MHW) is 147 cm, the highest high water (HHW) is 315 cm, the lowest low water (LLW) is −28 cm, the mean tidal range is 89 cm, and the maximum tidal range is 255 cm (China Nave Hydrographic Office, 2022).

The U-Th isotopic data of the three *in situ* fossil *Porites* corals (Fig. 4) from the east coast of Hainan Island are listed in Table S3. The measured U concentration ($\times10^{-6}$) was variable and ranged from (2.820 7 ± 2.2) $\times10^{-6}$ to (3.167 7 ± 2.3) $\times10^{-6}$, with an average value of 2.997 9 $\times10^{-6}$. The values of the initial δ^{234}U (T) varied between (147.2 ± 1.1)‰ and (151.2 ± 1.4)‰ (2σ, similarly hereafter), which were within the range for modern seawater (144 ± 2)‰ (Chen et al., 1986) and modern corals (156 ± 6)‰ (Stirling et al., 1995). Correspondingly, the six U-Th dating ages of our three *in situ* dead *Porites* ranged from (5 314 ± 14) cal a BP to (3 485 ± 16) cal a BP (years before 1950, similarly hereinafter), thus spanning 1829 years (Table S3). These dates have 2σ errors of ± 14 years to 27 years.

Additionally, over 360 published U-Th ages for the *in situ* dead *Porites*, *Porites* microatolls, branching corals, and coral-related debris were collected, although only 273 coral U-Th ages were finally selected after recalculation and reliability assessment. Therefore, a total of 276 coral U-Th ages, including our six new data points, were selected and compiled in this study.

Distribution of the δ^{234}U (T) variations (Fig. 5a), the U concentrations (Fig. 5b) and U-Th ages (Fig. 5c) as shown in Fig. 5 (Table S4). Their δ^{234}U (T) values varied from (143.7 ± 1.6)‰ to (156 ± 3)‰ with an average of 147.28‰, which was generally comparable to those of modern corals (Stirling et al., 1995) and seawater (Chen et al., 1986). The U concentrations was 3.072 1 × 10^{-6} on average, ranging from 1.872 $\times10^{-6}$ to 4.163 9 $\times10^{-6}$. Accordingly, those ages ranged from (7 463 ± 37) cal a BP to (−67 ± 2) cal a BP, with a 2σ error from ± 1 year to 319 years, thus spanning ~7 500 years.

4.4 *Episodic reef growth*

The 276 coral U-Th ages, including our six new data points, ranged from (7 463 ± 37) cal a BP to (−67 ± 2) cal a BP (Figs 5c, d, Table S4) and provided unique insights into past coral development, responses to recent disturbance regimes, and potential for future reef growth. The average two standard deviation of the determination errors (± 2σ) of all 276 U-Th ages was approximately 49.70 years. For this study, an average 50-year interval was used to categorize the coral U-Th ages; thus, a total of 57 intervals of more than 50 years with no coral U-Th age distributions but belong to 25 periods were identified. Furthermore, 40 gaps/hiatus were observed between two successive ages of more than 50 years with no coral U-Th age distributions, which were largely compatible with the previous 50 intervals. The 50 intervals were mainly distributed in the period of (7 463 ± 37) cal a BP to (7 062 ± 100) cal a BP (4 gaps), and the period of (4 103 ± 23) cal a BP to (650 ± 5) cal a BP (26 gaps). Based on the age distributions and the 50-year class interval, four distinguishable episodes punctuated by two switch-on episodes and two switch-off episodes were identified during the Holocene, as shown in Fig. 5d.

Figure 5d shows that episode 1 contained only 2 coral U-Th ages (0.72%), and it started at (~7 436 ± 37) cal a BP and lasted until (7 062 ± 100) cal a BP. This episode likely represents the initial time of coral development in this area. According to the criteria of 50-year class intervals, no coral U-Th ages were distributed in the following periods: before 7 500 cal a BP, (7 450–7 200) cal a BP and (7 150–7 100) cal a BP. Among those 276 U-Th ages, 140 coral U-Th ages (56.88%) fall into episode 2, which lasted approximately 2 800 years from (7 062 ± 100) cal a BP to (3 371 ± 21) cal a BP. This result indicates thriving coral growth in the Mid-Holocene, which formed the geomorphic pattern of modern coral reefs. Nevertheless, the U-Th ages can be sorted into 22 gaps between two successive ages of more than 50 years during this

Fig. 4. Images showing macro-structures and preservation status of Holocene fossil *Porites* corals on the east coastal Hainan in the northern SCS. The diameters in Images a, b and c are 101.5 cm, 253 cm, and 191 cm, respectively.

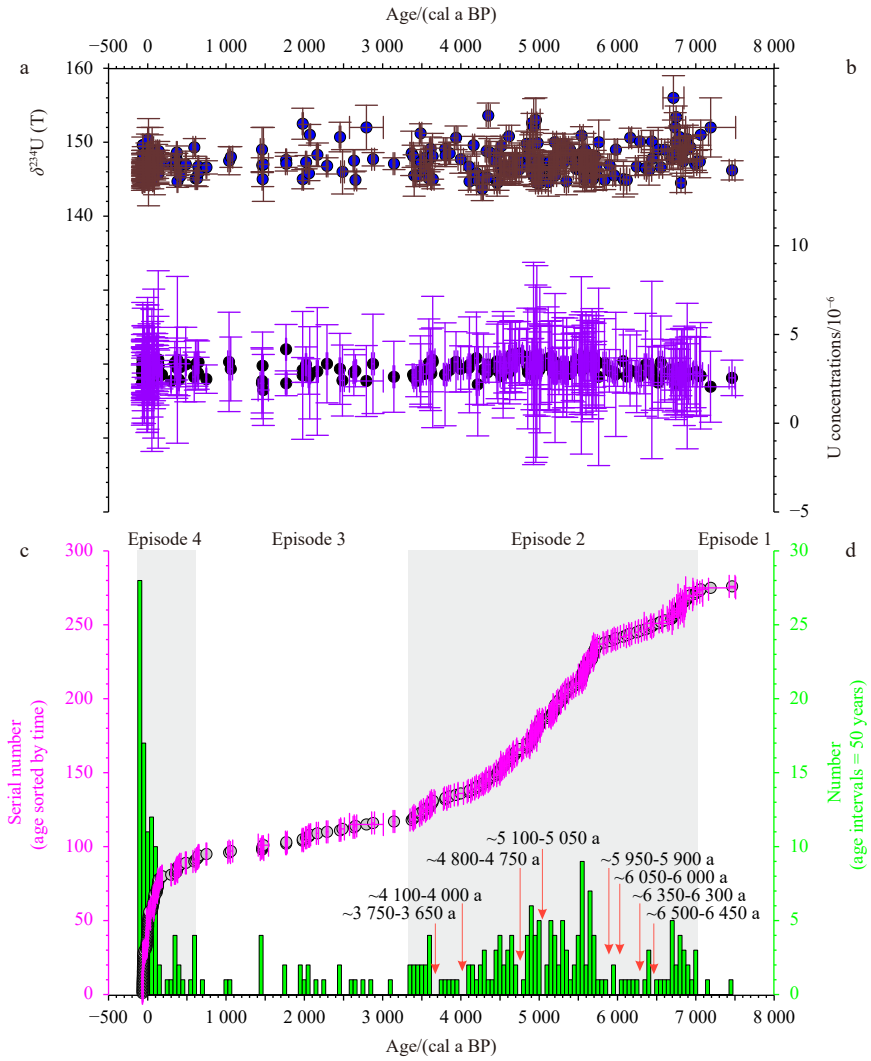

Fig. 5. Distribution of the δ^{234}U (T) variations (a), the U concentrations (b) and U-Th ages (c) for the 276 *in situ* dead *Porites*, *Porites* microatolls and coral-related debris from the northern SCS. Episodes of corals growth from the northern SCS during the Holocene based on the U-Th ages order and its' two standard deviations (50-year interval) of the age determination errors (±2σ) (d).

period, namely (6 992 ± 19) cal a BP to (6 937 ± 37) cal a BP, (6 686 ± 24) cal a BP to (6 603 ± 41) cal a BP, (6 603 ± 41) cal a BP to (6 553 ± 23) cal a BP, (6 519 ± 179) cal a BP to (6 445 ± 19) cal a BP, (6 359 ± 17) cal a BP to (6 287 ± 19) cal a BP, (6 246 ± 19) cal a BP to (6 162 ± 19) cal a BP, (6 075 ± 39) cal a BP to (5 979± 22) cal a BP, (5 958 ± 19) cal a BP to (5 897 ± 22) cal a BP, (5 897 ± 22) cal a BP to (5 935 ± 20) cal a BP, (5 935 ± 20) cal a BP to (5 760 ± 66) cal a BP, (5 304 ± 30) cal a BP to (5 253 ± 15) cal a BP, (5 116 ± 36) cal a BP to (5 021 ± 18) cal a BP, (4 850 ± 39) cal a BP to (4 750 ± 33) cal a BP, (4 613 ± 34) cal a BP to (4 561 ± 53) cal a BP, (4 436 ± 21) cal a BP to (4 369 ± 12) cal a BP, (4 272 ± 15) cal a BP to (4 216 ± 19) cal a BP, (4 162 ± 14) cal a BP to (4 110 ± 17) cal a BP, (4 103 ± 23) cal a BP to (3 998 ± 35) cal a BP, (3 998 ± 35) cal a BP to (3 938 ± 23) cal a BP, (3 938 ± 23) cal a BP to (3 804 ± 15) cal a BP, (3 799 ± 22) cal a BP to (3 641 ± 16) cal a BP. According to the 50-year class interval criterion, the above-mentioned gaps mainly centered on the intervals of (6 500–6 450) cal a BP, (6 350–6 300) cal a BP, (6 050–6 000) cal a BP, (5 950–5 900) cal a BP, (5 100–5 050)

cal a BP, (4 800–4 750) cal a BP, (4 100–4 000) cal a BP, and (3 750–3 650) cal a BP as shown in Fig. 5d. Similarly, episode 3 contained 23 coral U-Th ages (8.33%) and lasted approximately 2 740 years from (3 371 ± 21) cal a BP to (650 ± 5) cal a BP [(1420 ± 23) BCE–(1300 ± 5) CE]; additionally, over 13 turn-off phases were observed, which mainly centered on (3 350–3 150) cal a BP, (3 100–2 900) cal a BP, (2 850–2 800) cal a BP, (2 750–2 700) cal a BP, (2 600–2 500) cal a BP, (2 450–2 300) cal a BP, (2 250–2 200) cal a BP, (2 150–2 100) cal a BP, (1 950–1 800) cal a BP, (1 750–1 500) cal a BP, (1 450–1 100) cal a BP, (1 000–750) cal a BP, and 700–650) cal a BP. Similar to episode 2, episode 4 also featured a large distribution of U-Th dating ages, indicating the occurrence of reef growth during the last millennia. Episode 4 consisted of 94 coral U-Th ages (34.06%) within the period of (650 ± 5) cal a BP to (−67 ± 2) cal a BP [(1 300 ± 5) CE–(2 017 ± 2) CE], thus spanning approximately 600 years, and it indicated the formation of the modern coral reef geomorphologic framework. However, coral U-Th ages were not obtained in the periods of (550–500) cal a BP (1400–1450 CE) and (250–200) cal a BP (1700–1750 CE).

4.5 *Age elevation*

The three *in situ* fossil *Porites* corals collected from the east coast of Hainan Island were analyzed for elevation measurements and U-Th dating. Elevation data indicate a difference of (35.69–71.09) cm between historical levels and the modern MSL if the influence of tectonic uplift is not considered. Based on the newly defined indicative meanings (which were derived from the 27 live *Porites* corals), the height of the top surface of the *in situ* fossil corals (H_{fossil}), and the height corrected for tectonic uplift ($H_{tectonic}$), 6 new SLIPs and 19 recalculated SLIPs were produced for historical sea-level reconstruction (as seen in Table S3). Additionally, the elevation error of the newly added coral sample was 8.33 cm, as indicated by the 27 modern live *Porites* corals. The measuring instrument error of the RTK GPS was 5 cm, and the sampling error was 1 cm, thus, the total sea-level error of our new SLIPSs was ± 9.8 cm. Accordingly, the sea-level indicators are plotted in a time-altitude graph with the range of errors, as shown in Fig. 6. The 6 new and high-quality SLIPs were dated from (5 314 ± 14) cal a BP to (3 485 ± 16) cal a BP and indicated a decrease in relative sea level (RSL) from (198.33 ± 9.8) cm to (169.33 ± 9.8) cm MTL (similarly hereinafter). While the 19 recalculated SLIPs indicated the RSL during the period of (5 393 ± 25) cal a BP to (3 390 ± 12) cal a BP was (227.7 ± 9.8) cm to (154.88 ± 9.8) cm MTL.

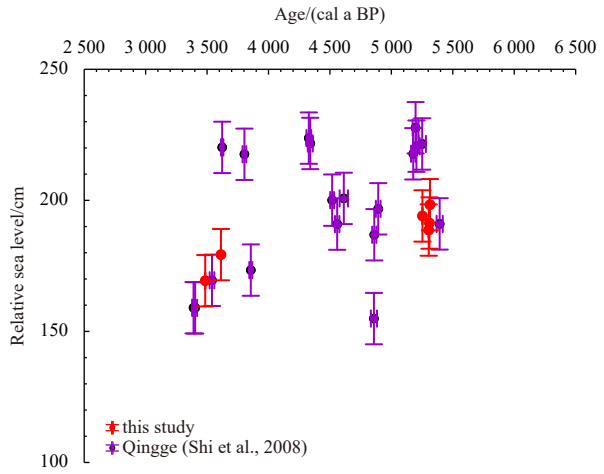

Fig. 6. U-Th age-elevation data for our 6 new SLIPs and 19 recalculated SLIPs from east costal Hainan Island in the northern SCS. Vertical uncertainties are uniformly ± 9.8 cm (±2σ).

After the elevations of the 6 new and 19 published SLIPs are adjusted by the indicative meanings and their ages were recalibrated, a time elevation RSL is produced as shown in Fig. 6. Overall, the 25 SLIPs indicated an RSL fluctuation between (227.7 ± 9.8) cm to (154.88 ± 9.8) cm from (5 393 ± 25) cal a BP to (3 390 ± 12) cal a BP. In detail, five stages of sea-level fluctuations can be identified from the distribution pattern of the age spectrum during the following periods. For instance, five SLIPs revealed that the sea level was (192.68 ± 9.8) cm between (5 393 ± 25) cal a BP and (5 253 ± 15) cal a BP. Four SLIPs revealed that the sea level was (221.91 ± 9.8) cm between (5 251 ± 30) cal a BP and (5 178 ± 18) cal a BP. Six SLIPs revealed that the sea level was (188.38 ± 9.8) cm between (4 893 ± 19) cal a BP and (4 518 ± 16) cal a BP. Five SLIPs revealed that the sea level was (211.32 ± 9.8) cm between (4 340 ± 20) cal a BP and (3 625 ± 10) cal a BP. Five SLIPs revealed that the sea level was (167.22 ± 9.8) cm between (3 613 ± 10) cal a BP and (3 390 ± 12) cal a BP.

5 Discussion

The high precision and accuracy of U-Th dating with a quantifiable vertical relationship to a reference tidal level enabled the reconstruction of both the time and trajectory of local sea-level fluctuations, and such dating also aids in understanding the responses of coral reef development to environment and climate change. In this study, we collected and analyzed three *in situ* fossil *Porites* corals from the east coast of Hainan Island in the northern SCS, from which six new and high-quality SLIPs were generated. The new data indicated that the RSL fluctuation ranged from (227.7 ± 9.8) cm to (154.88 ± 9.8) cm after tectonic correction in the SCS during the Middle to Late-Holocene. This finding adds to the debate on whether a higher Mid-Holocene sea-level highstand occurred. Coupled with an additional 270 published coral U-Th ages, our findings enabled the recognition and precise timing of different phases of coral reef initiation, growth, and turn-off during the Holocene as well as their relationship with climate change.

5.1 *Implications for Mid-Holocene sea levels*

Elevations of the upper limit of coral growth have been determined for 27 modern *Porites* corals from Tongguling along the coast of Wenchang, Hainan Island. These corals appear to have had a planar upper surface typical of the microatoll growth form. Such a growth form is important because it implies that LLW constrained the upward growth of the coral. Corals that do not have such an upper flat surface may not be limited by low water levels and therefore are not indicators of former sea levels. Furthermore, the *Porites* habitat along the east coast Hainan Island lie at (−43.09 ± 9.8) cm in elevation, which is largely comparable with that observed for microatolls (−30.02 ± 16.2) cm from Cocos Island (Smithers and Woodroffe, 2000). This finding suggested that the conditions for establishing a close relationship between the upper coral growth limit and sea level are very good and indicated that live *Porites* corals is a precise diagnostic sea-level indicator, and therefore serves as a modern sea-level indicator in this study. Typically, microatolls include a single colony of massive *Porites* up to several meters in diameter, and reef flats are commonly formed by the dead upper surfaces of *in situ* massive *Porites*. Accordingly, it is reasonable to infer that any height changes in the upper surfaces/rims of different ages within an individual *Porites* in a relatively stable tectonic area should

reflect sea-level variation.

The study area lies further away from the plate boundary and has been regarded as relatively stable tectonically (Zhao, 1983; Huang et al., 1995; Zong, 2004), although a tectonic uplift rate of (0.02–0.05) mm/a has been reported from the coral reef area in Leizhou Peninsula in the northern SCS since the Holocene (Yu et al., 2002; Zhan et al., 2007), which is much lower than the growth rate of coral reefs (1 mm/a). Therefore, combined with the elevations of dated *in situ Porites* (microatolls), we inferred that the large *in situ* fossil *Porites* (microatolls) exposed at MTL from the northern SCS were not the product of tectonic uplift. Rather, a plausible interpretation for this situation is the contemporaneous high sea level. In other words, the micro-geomorphology of these *in situ* fossil *Porites* (microatolls) suggested that the elevation differences between the upper surfaces mainly resulted from sea-level variations. Additionally, an earthquake occurred in 1 605 in Puqian (Hainan Island) that resulted in a large subsidence range in the outer bay of Puqian Bay and a small subsidence range in the inner bay with obvious spatial differences (Zhang et al., 2008), and it would lead to a lowering of the sea level without a need for any RSL change. Although this situation is feasible, we consider it unlikely because tidal adjustments would likely manifest as a more gradual change in the RSL curve, which is not the case in our previous study (Yue and Tang, 2023). Overall, the tectonically corrected sea level presented an average 16.05 cm decrease relative to the current record (Table S3). Greater differences were observed with age, and vice versa.

In theory, the RSL should increase in the far-field due to a small amount of ice melting after the final melting of the Laurentide and Fennoscandian ice sheet between 7 000 cal a BP and 4 000 cal a BP (Lambeck et al., 2014; Bradley et al., 2016). In this study, six new SLIPs and the recalibration of the previously published SLIPs were generated for tectonic correction and reliability analysis. As shown in Fig. 6, the corrected ages and altitudes of the SLIPs were plotted. It showed that the reconstructed RSL was was (192.68 ± 9.8) cm MTL between (5 393 ± 25) cal a BP and (5 253 ± 15) cal a BP, followed by a rise to (221.91 ± 9.8) cm between (5 251 ± 30) cal a BP and (5 178 ± 18) cal a BP, and decline to (188.38 ± 9.8) cm between (4 893 ± 19) cal a BP and (4 518 ± 16) cal a BP, then rise to (211.32 ± 9.8) cm between (4 340 ± 20) cal a BP and (3 625 ± 10) cal a BP, and finally fall to (167.22 ± 9.8) cm between (3 613 ± 10) cal a BP and (3 390 ± 12) cal a BP. Comparison between the sea level derived from the 6 new SLIPs and 19 recalculated SLIPs and the predictions of the glacial isostatic adjustment (GIA), e.g., ICE-4G model (Wang et al., 2012) and the outputs of the final ice-volume equivalent sea level (ESL) model from Bradley et al. (2016) offer us an opportunity to infer causal mechanisms of the Mid-Holocene sea-level history.

As shown in Fig. 7a, the reconstructed sea-level elevations were roughly consistently along the predicted Mid-Holocene sea level, which were above the ICE-4G model predictions but below the output of ESL model. These reconstructed sea-level and predicted elevations may imply a significant regional uplift due to neo-tectonic movement. Alternatively, a greater amount of ice melting is required for the Mid-Holocene period. For instance, considering the northern SCS is located near the active subduction zone, the mantle viscosity coefficient is low, and the melted ice water is significantly affected by weak viscosity regions, which produced faster response rate in the middle Holocene crustal activity, thus reducing the RSL (Bradley et al., 2016). Over all, this likely suggested that both GIA and ESL exerted a significant influence in the RSL history in this far-field region. Additionally, we noted that this is contrary to Malay Peninsula (Tam et al., 2018), which is comparable with the GIA model results. It was likely considered as the differential responses caused likely by the difference in the upper mantle viscosity between these two landmasses (Xiong et al., 2020), or refinements are needed in ice-history models to fully capture our RSL data.

5.2 *Regional correlation and difference analysis of sea level*

The results from the east coast Hainan Island indicated that the RSL was (227.7 ± 9.8) cm to (154.88 ± 9.8) cm between (5 393 ± 25) cal a BP and (3 390 ± 12) cal a BP recorded by the *in situ* fossil massive *Porites* corals. It further testified to the existence of a higher Mid-Holocene sea-level highstand in the northern SCS. Indeed, this scenario was generally consistent with other findings from the coast surrounding the SCS, although a certain degree of variability was observed in the timing and the height varied according to location.

For instance, both the U-Th and ^{14}C ages for *Porites* corals and *Porites* microatolls records collected from the coastal Lei-Qiong area in the northern SCS indicated a (100–400) cm higher sea level above the modern MSL during the Mid-Holocene (Nie et al., 1996; Zhao and Yu, 2002; Huang et al., 2007; Shi et al., 2008; Yu et al., 2009; Yao et al., 2013). Additionally, evidence for a Holocene transgression was recorded in Thailand and Vietnam between 8 000 cal a BP and 7 000 cal a BP, and it reached a peak value close to 150 cm around 6 000 cal a BP (Tanabe et al., 2003; Stattegger et al., 2013). Similar patterns have been observed by comparison with distal records, e.g., the RSL was between 140 cm and 300 cm above present values along the east coast of Peninsula Malaysia at 7 000 cal a BP (Parham et al., 2014), and it then reached 150 cm around 6 500 cal a BP (Zhang et al., 2021). Similar patterns were also observed in Belitung Island, Indonesia, on the Sunda Shelf, where a Mid-Holocene highstand of 180 cm occurred between 6 800 cal a BP and 6 600 cal a BP (Meltzner et al., 2017). Recently, highstand sea-level observation data were reported for the period of (6 100–6 000) cal a BP along the western Sarawak coast of Borneo (Majewski et al., 2018). Besides, a case in point is the sea level around 5 140 cal a BP (uncorrected ^{14}C age) in the Hongkong was about 190 cm higher than the present-day was reported (Davis et al., 2000). Similar patterns were also observed in the Penghu Islands, where indicated a highest Holocene RSL about 240 cm above the present sea level at about 4 700 years ago (Chen and Liu, 1996). Even a level of approximately (3 ± 2.5) m above the present mean sea level was recorded from corals in Ishigaki Island at around 5 000 cal a BP (Hongo and Kayanne, 2010).

The above-mentioned past sea level records indicated that the formation and appearance of the Mid-Holocene sea-level highstand in the northern SCS was basically synchronous with the surrounding areas of the SCS. In addition, the tropical Pacific Ocean (Dickinson, 2004), east coast of India from Cape Comorin to Rameswaram (Banerjee, 2000), South Africa coastline (Ramsay, 1996), and southern Brazil (Angulo et al., 1999) have also confirmed the existence of a Mid-Holocene highstand sea-level, which suggests that the regional changes in RSL were unprecedented in modern times.

What's more, we noted that sea-level reconstructions based on different methods or criteria presented significant differences and uncertainties and were not comparable in terms of the time, phasing, and amplitude of the highstand. In terms of dating methods, the radiocarbon content of terrestrial organisms differs from that of marine organisms due to the effect of the marine carbon pool (Hall and Henderson, 2001), and a difference of approximately 400 years in radiocarbon age has been observed between

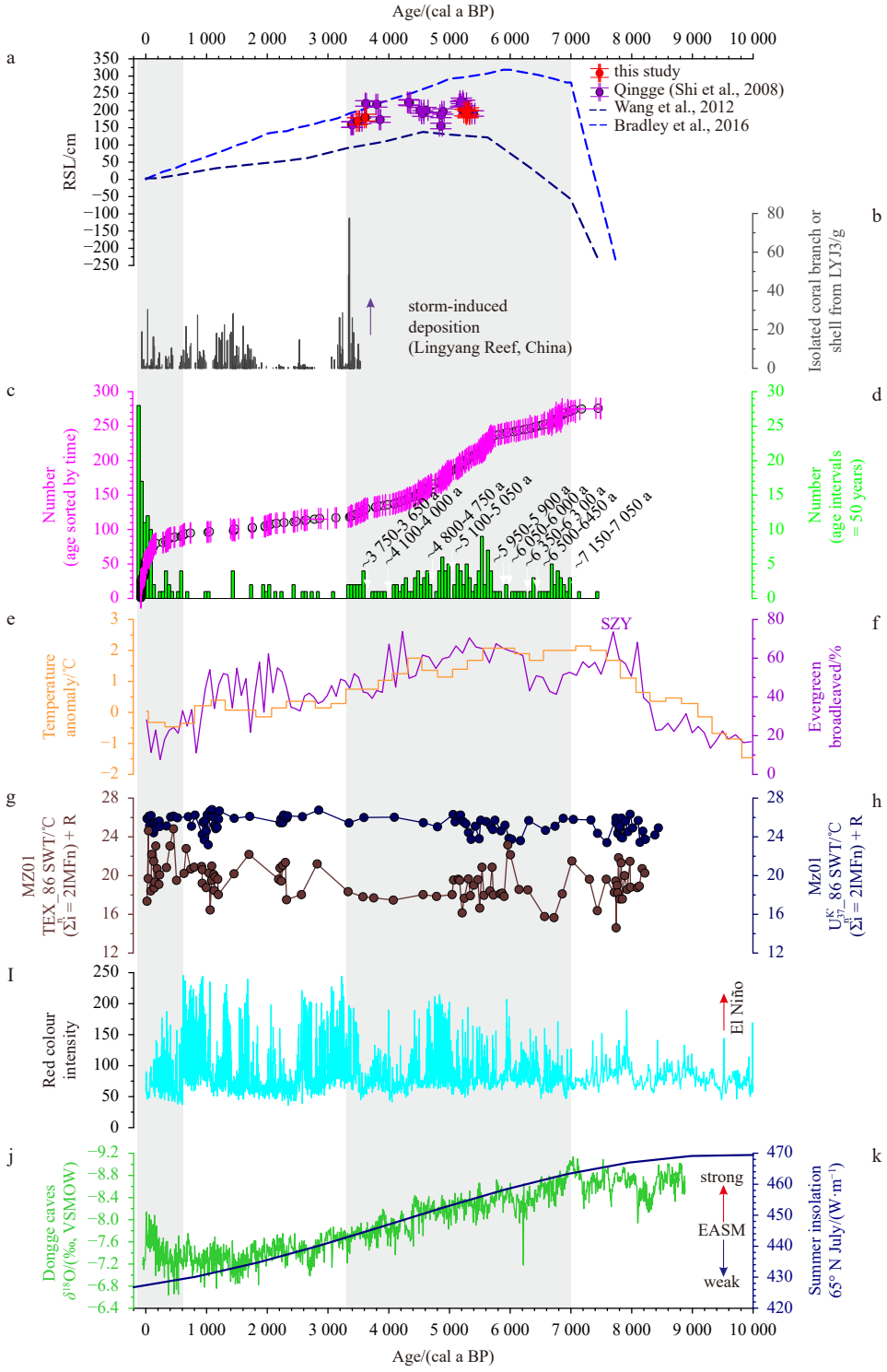

Fig. 7. Comparison of Mid-Holocene RSL data with the predictions of the ICE-4G model (Wang et al., 2012) and the outputs of the final ice-volume equivalent sea-level model from Bradley et al. (2016) (a), storm records from Lingyang Reef (Yue et al., 2019) (b), coral U-Th ages distribution pattern derived from the *in situ* dead corals on the coast of northern SCS (c, d), the reconstructed temperature (relative to the present) from China (Wang and Gong, 2000) (e), subtropical evergreen broadleaved percentage (Yue et al., 2012) (f), the sea surface temperatures (SSTs) of Core MZ01 from the continental shelf of the East China Sea (Pan et al., 2020) (g, h), reconstruction of El Niño occurrences from Laguna Pallcocha, Ecuador (Moy et al., 2002) (i), δ ^{18}O records (‰, VSMOW) from the stalagmite of Dongge Cave (Wang et al., 2005) (j), and the 65°N summer insolation in July in the Northern Hemisphere (Berger and Loutre, 1991) (k).

terrestrial and marine organisms of the same age. Additionally, ^{14}C dating of coral provides dates that are (~200–1 000) years younger than their corresponding U-Th dating ages due to spatial and temporal variability in the marine reservoir effect as well

as the influence of the surrounding environment and late diagenesis (Eisenhauer et al., 1993; Ingram and Southon, 1996; Yu et al., 2002, 2010; Bard et al., 1993, 1998; Hua et al., 2020). Moreover, the carbon pool effect has different effects in different time periods (Yu et al., 2010).

In terms of reconstruction methods, values at 100 cm below the tidal datum (Nie et al., 1996) or the mean lower low water of the local gauge station (Yao et al., 2013) were defined as the upper limit of coral growth. Even the elevation data were expressed in terms of altitude without providing any datum plane or reference to the upper surface of modern live *Porites* corals and the *Porites* microatolls (Shi et al., 2008; Yu et al., 2009). These findings suggest that the quantifiable vertical relationship of a sea-level indicator to a reference tidal level, i.e., indicative meaning, was not a quantifiable or uniform criterion, which may be the main reason for the different sea-level histories for the same region. Thus, controversies regarding sea-level changes will inevitably arise. For instance, the indicative meaning of the 27 live *Porites* corals in this study can be expressed as (146.09 ± 9.8) cm below MTL (comparing the height with tidal ranges of nearby Qinglan tide gauge), or 15.09 cm below LLW, even (–43.09 ± 9.8) cm (relative to 1985 National Elevation Benchmarks). Significantly, it corresponds to a reconstructed RSL of (227.7 ± 9.8) cm to (154.88 ± 9.8) cm MTL, or (81.61 ± 9.8) cm to (8.79 ± 9.8) cm between (5 393 ± 25) cal a BP and (3 390 ± 12) cal a BP as shown in Fig. 5. Obviously, based on different criteria, the same sea-level indicators, e.g., our 6 new and 19 recalculated SLIPs, support the following different findings: no obvious higher-than-present sea-level highstand or higher sea-level highstands in the mid-late Holocene is found from the northern SCS. In any case, our analysis demonstrates that mid-late Holocene sea-levels highstand did exist.

In addition, age and vertical errors (Yue and Tang, 2023), differential GIA (Xiong et al., 2020), and vertical tectonics (Yao et al., 2013) should be considered as significant factors in sea-level reconstruction, although the study area is in a relatively tectonically stable region on the northern coast of the SCS (Zhao, 1983; Huang et al., 1995; Lu, 1997; Zong, 2004).

5.3 *Possible influences on coral reef growth*

The worlds coral reefs are increasingly impacted by natural climatic and environmental change and anthropogenic disturbance; thus, understanding historical causes and mechanisms of reef switch-on and switch-off states is of critical importance (Perry and Smithers, 2011; Yan et al., 2019). Reports have indicated that the initiation of coral reefs and evolutionary states (switch-on and switch-off) reflect the long-term synergistic effects of several factors, e.g., sea-level fluctuations and climate change (Montaggioni, 2005; Yu et al., 2012; Foster and Attrill, 2021). However, their potential to influence the state of reef-building at timescales meaningful to contemporary reef ecology are poorly documented. Therefore, to identify possible climatic and environmental drivers of switch-on and switch-off events, we compared coral age distributions to regional paleoenvironmental conditions during the Holocene, such as the reconstructed RSL (Fig. 7a), storm records from Lingyang Reef (Yue et al., 2019) (Fig. 7b), the reconstructed temperature (relative to the present) from China (Wang and Gong, 2000) (Fig. 7e), subtropical evergreen broadleaved percentage (Yue et al., 2012) (Fig. 7f), the sea surface temperatures (SSTs) of Core MZ01 from the continental shelf of the East China Sea (Pan et al., 2020) (Figs 7g, h), reconstruction of El Niño occurrences from Laguna Pallcocha, Ecuador (Moy et al., 2002) (Fig. 7i), δ^{18}O records (‰, VSMOW) from the stalagmite of Dongge Cave (Wang et al., 2005) (Fig. 7j), and the 65°N summer insolation in July in the Northern Hemisphere (Berger and Loutre, 1991) (Fig. 7k).

Based on the distribution of coral U-Th ages, it can be inferred that the development of coral reefs in the northern SCS experienced initial development, boom growth, bust decline, and flourishing development again. For instance, our dataset clearly demonstrated a distinct period (Episode 1) between before (7 062 ± 100) cal a BP during the early Mid-Holocene when coral reefs on the northern SCS experienced the first switch-on phase (Figs 7b, c). Significantly, there is evidence that a period of rapid rise of RSL from (–49.3 ± 0.8) m to the present height occurred from 10 500 cal a BP to 7 000 cal a BP (Xiong et al., 2018). We thus inferred that coral reefs initially developed in the northern SCS at the onset of the Mid-Holocene as a response to progressive transgression of the shelf associated with the postglacial sea-level rise (Zong, 2004; Zong et al., 2012; Xiong et al., 2018), although the coral ages were sporadically prsented. As the decay of ice sheets and glaciers caused post-glacial sea-level rise during this interval of global warming (Clark et al., 2012) and marine inundation occurred across the extensive upper continental selves (Smith et al., 2011), favorable conditions were provided for the development of reef in the Lei-Qiong area along the northern SCS. Additionally, increases of temperature (Wang and Gong, 2000) and a high percentage of subtropical pollen assemblages (Yue et al., 2012) in the early Holocene (as shown in Figs 7e, f) also suggested an interval of global warming and warm climate that favored the initiation of coral reef in this area. At the same time, contemporaneous records of coral widely distributed in Malaysia and other places (Dickinson, 2004; Horton et al., 2005; Majewski et al., 2018) likely indicate a universal development stage of coral reefs during this period.

Compared with the last glacial-interglacial cycle, the Mid-Holocene has been known as a brief period of relative stable climate, which included a stabilized sea-level and warmer SST stage (Gagan et al., 1998; Stott et al., 2004). *In situ* massive corals and branching corals were extensively distributed on the reef flat at Lei-Qiong, as shown in episodes 2 and 4, indicating that coral species have increased significantly. Of particular significance is episode 2, which mainly centered on the period (7 062 ± 100) cal a BP to (3 371 ± 21) cal a BP (Figs 7b, c). Firstly, it basically overlaps the Mid-Holocene sea-level highstand predicted by the ICE-4G model (Lambeck et al., 2014; Bradley et al., 2016) and recorded by our high-precision U-Th dating SLIPs, as shown in Fig. 7a. With this in mind, we are convinced that the Mid-Holocene was optimal for coral growth, and such growth was generally well correlated to the stabilization and culmination of the post-glacial global sea level (Zhao and Yu, 2002). In addition, the flourishing of corals in episode 2 almost perfectly corresponds to the Holocene thermal maximum (HTM). As shown in Fig. 7k, this period well coincided with a high stage of summer insolation at 65°N (Berger and Loutre, 1991). Higher temperatures (relative to the present) from China (Wang and Gong, 2000) and SST records from western tropical Pacific (Stott et al., 2004) indicated a rapid warming scene. Nearby SST records during the period of 6 500 cal a BP to 6 100 cal a BP derived from *Porites* corals in Sanya indicated that the average minimum winter and maximum summer monthly SSTs were approximately (0.5–1.4℃) and (0–2.0℃) higher than at present in the northern SCS (Wei et al., 2007). This finding suggested that warm winters are occurring more frequently while the warm climate favors thriving coral in this area and is probably conducive to the formation of a stable coral reef ecosystem.

Moreover, the switch-on episode is also consistent with other records from the subtropical zone, such as the high percentage of subtropical pollen record of SZY in Fujian (Yue et al., 2012) (Fig. 7f). As shown in Fig. 7j, the δ^{18}O record of speleothem and broader syntheses identified a strengthening of the EASM (Dykoski et al., 2005; Wang et al., 2005; Cai et al., 2021) induced by the strong insolation forcing a northward migration of the ITCZ (Haug et al., 2001). The monsoon circulation caused by the enhancement of solar radiation in the Northern Hemisphere reached the strongest stage during the period of ~9 000 cal a BP to 6 000 cal a BP (Sirocko et al., 1993). Furthermore, episode 2 formed prior to the weakening of EASM (Dykoski et al., 2005; Wang et al., 2005) and was also well correlated with the stronger ENSO activities (Moy et al., 2002), as seen in Fig. 7i. Moreover, the latest research points out that the shrinkage of the EAWM is associated with increased ENSO events since the Mid-Holocene (Wu et al., 2019). Consequently, the strengthening of the EASM drives more warm water masses northward, which is beneficial for coral migration to high latitude areas. For example, in our dataset, the number of coral U-Th ages from Weizhou Island and Leizhou Peninsula at relative high latitudes in Episode 2 and 4 increased significantly, which may be a positive response to these climate changes. On the contrary, the strengthening of the EAWM drives colder coastal currents southward, results in cooler winter SST and a larger SST seasonality, which inhibits the growth of corals, as seen in episode 3. Except that, it is reported that typhoon caused significant damage to reef associated depths on the passage of the atoll, where currents generated by the typhoon produced the strongest energy (Yang et al., 2015). After storm surges as seen in Fig. 7b (Yue et al., 2019), significantly fewer corals were recorded as seen in Episode 3, likely suggesting that the storm surge disrupted coral growth and inhibited reef development. Therefore, it must be emphasized that climate change can potentially impact coral reefs through several key mechanisms, such as sea-level rise, SST (rising global temperatures), ENSO, EASM and storm surges, although it is tempting to ascribe such changes to a single environmental cause.

5.4 *Implications for climate events*

However, it must be pointed out that the HTM was influenced by climatic cooling events. For example, the well-documented δ^{18}O records from stalagmites from Dongge Cave (Dykoski et al., 2005; Wang et al., 2005) and ice core records indicate the weakening of the EASM (Rasmussen et al., 2006). Reef corals are well-known as excellent archives for recording the climatic and environmental history of tropical oceans because corals growing at their latitudinal limits may be the most sensitive to global climatic changes (Yu, 2012). Many organisms tend to be limited to specific thermal ranges (Drinkwater et al., 2010). SST is a primary controlling factor of coral reef distribution and coral reef ecosystems (Yu, 2000; Lough, 2012). It is worth noting that higher winter SSTs would favor the development of coral reef ecosystems (Yu, 2000). On the contrary, cold winter SSTs caused a decrease and/or cessation of coral skeletal extension (Fallon et al., 1999). Therefore, it is reasonable to infer that the coral growth hiatuses that occurred in episodes 1 and 2 during the Mid-Holocene, as observed from the northern SCS based on the criteria of 50-year class intervals, should be a response to cooling events. Coincidentally, the timing of these reef growth disturbance with hiatuses were generally consistent with the above multiple cooling events recorded in stalagmites (Dykoski et al., 2005; Wang et al., 2005; Cai et al., 2021) when the gaps/hiatuses between two successive ages more than 50 years were considered.

Additionally, as shown in Fig. 1, this area is not only greatly affected by the EAWM and coastal current but also suffered cool water intrusions in winter and received inputs mainly from the Pearl and local rivers and coastal runoff. Cold coastal current and/or terrestrial inputs from nearby rivers that may bring more suspended sediments likely further prevent the growth of coral reefs. Furthermore, a detailed ecological, micro-structural, and skeletal Sr/Ca study from Leizhou Peninsula suggested high-frequency winter cooling and reef coral mortality during the period (7 500–7 000) cal a BP (Yu et al., 2004), which was comparable to the strong upwelling intensity during this period and almost synchronous with the hiatus of coral growth. Importantly, a similar pattern was also observed in Kodakara Island in the northwestern Pacific (Hamanaka et al., 2012) as well as Ovalau and Moturiki islands in Fiji in the southwest Pacific (Nunn, 2000). As shown in Fig. 7, the periods of (7 150–7 100) cal a BP, (6 500–6 450) cal a BP, (6 350–6 300) cal a BP, (6 050–6 000) cal a BP, (5 950–5 900) cal a BP, (5 150–5 000) cal a BP, (4 800–4 750) cal a BP, (4 100–4 000) cal a BP and (3 750–3 600) cal a BP corresponded particularly well to the rapid decline of SST and subsurface water temperature (Pan et al., 2020) and further emphasized that the weakening EASM induced by insolation forced a southward migration of the ITCZ in the Northern Hemisphere (Haug et al., 2001). Therefore, a plausible interpretation for the cessation of the developmental stage or the switch - off period was the cold events that occurred during those periods within Mid-Holocene. Meanwhile, they also appeared to be synchronous with North Atlantic Holocene cooling events 3–4 (Bond et al., 1997, 2001); thus, they likely have a global connection.

Nonetheless, other interpretations appear to be persuasive, such as the rapid sea-level rise outpacing reef growth (Webster et al., 2018) and abrupt decline leading to subaerial exposure. Regional common causes may also have had an influence, such as coral bleaching during ENSO warm phases on inter-annual time scale or during positive PDO phases or sharp phase transitions on interdecadal time scales (Yu et al., 2012), increased nearshore deposition of terrigenous sediment, which may be related to increased tropical-cyclone frequency and intensity or early human activities (Nunn, 2000), and unknown local factors. Finally, it is also difficult to rule out the omission of sampling. After all, only 276 U-Th ages have been compiled; thus, including all *in situ* coral samples in this area is difficult.

6 Conclusions

This study has reconstructed the Mid-Holocene relative sea-level history in the relatively tectonically stable northern SCS with two specific objectives: quantifying the sea-level indicative meanings of *Porites* corals and producing new high-quality SLIPs. In this study, we surveyed the growth range of 27 modern live *Porites* and reported six newly added U-Th-dated SLIPs derived from three *Porites* along the east coast of Hainan Island in the northern SCS. The investigations showed that the top surface elevations of those live *Porites* are (146.09 ± 9.8) cm below MTL or 15.09 cm below LLW, (–43.09 ± 9.8) cm and almost horizonal in a narrow range, which suggested that their upward growth limit is constrained by the sea level, and the LLW is the highest level of survival for the modern live *Porites* corals. It further suggested that *Porites* coral is a precise diagnostic sea-level indicator that can provide a firmer basis for extrapolating historical sea levels. Additionally, based on the newly defined indicative meanings, the six new SLIPs coupled with 19 recalculated SLIPs indicated that the RSL varied from (227.7 ± 9.8) cm to (154.88 ± 9.8) cm above MTL during in the period of (5 393 ± 25) cal a BP to (3 390 ±

12) cal a BP, which provided support for the existence of Mid-Holocene sea-level highstands in the northern SCS. This scenario was generally consistent with other findings from the coast surrounding SCS, and indicates that the formation and appearance of the sea-level highstand in the northern SCS in the Mid-Holocene was synchronous with that in the surrounding areas of the SCS, which likely presented a local background. Furthermore, regional correlations and difference analyses of the reconstructed sea levels suggested that the quantifiable vertical relationship of the sea-level indicator to a reference tidal level, which represents indicative meaning, was not a quantifiable or uniform criterion and thus may represent the main reason for different sea-level histories for the same region. Thus, controversies about sea-level changes will inevitably arise.

Moreover, our six new data points coupled with the additional 270 coral U-Th ages depicted a history of coral reef development in the northern SCS during the Holocene, which experienced initial development [before (7 062 ± 100) cal a BP], boom growth (7 062 ± 100) cal a BP to (3 371 ± 21) cal a BP, bust decline (3 371 ± 21) cal a BP to (650 ± 5) cal a BP and flourishing development again [since (650 ± 5) cal a BP]. Furthermore, 56.88% of the coral U-Th dating ages fell in the Mid-Holocene, suggesting a peak period of coral reef development that was probably associated with a relatively stable period of sea level and the Holocene thermal optimum. Comparisons with the other climate records indicated that climate change can potentially impact coral reefs through several key mechanisms. For instance, the strengthening of EASM drives more warm water masses to move northward, which is beneficial for coral migration to high latitude areas and the boom growth of coral reef. On the contrary, the bust decline of coral reef featured by reef growth disturbance with hiatuses during the Mid-Holocene broadly corresponded with the synergistic effects of synchronous low temperature and rapid global cooling events. In summary, we inferred that the development/cessation of coral reef in the northern SCS was probably closely associated with the dry and cold climate in South China, which was reflected in the synchronous strengthening/weakening of the ENSO and EASM induced by the 65°N summer insolation, which forced the migration of the ITCZ.

Acknowledgements

We thank Tingli Yan for assistance in the fieldwork and samples collection. We are thankful to the editor, and the anonymous reviewers for their constructive comments and suggestions.

References

Anderson T R, Fletcher C H, Barbee M M, et al. 2015. Doubling of coastal erosion under rising sea level by mid-century in Hawaii. Natural Hazards, 78(1): 75–103, doi: 10.1007/s11069-015-1698-6

Angulo R J, Giannini P C F, Suguio K, et al. 1999. Relative sea-level changes in the last 5500 years in southern Brazil (Laguna–Imbituba region, Santa Catarina State) based on vermetid ^{14}C ages. Marine Geology, 159(1-4): 323–339, doi: 10.1016/S0025-3227(98)00204-7

Banerjee P K. 2000. Holocene and Late Pleistocene relative sea level fluctuations along the east coast of India. Marine Geology, 167(3-4): 243–260, doi: 10.1016/S0025-3227(00)00028-1

Bard E, Arnold M, Fairbanks R G, et al. 1993. ^{230}Th-^{234}U and ^{14}C ages obtained by mass spectrometry on corals. Radiocarbon, 35(1): 191–199, doi: 10.1017/S0033822200013886

Bard E, Arnold M, Hamelin B, et al. 1998. Radiocarbon calibration by means of mass spectrometric ^{230}Th/^{234}U and ^{14}C ages of corals: an updated database including samples from Barbados, Muruoa and Tahiti. Radiocarbon, 40(3): 1085–1092, doi: 10.1017/S0033822200019135

Barkley H C, Cohen A L, Mollica N R, et al. 2018. Repeat bleaching of a central Pacific coral reef over the past six decades (1960–2016). Communications Biology, 1: 177, doi: 10.1038/s42003-018-0183-7

Berger A, Loutre M F. 1991. Insolation values for the climate of the last 10 million years. Quaternary Science Reviews, 10(4): 297–317, doi: 10.1016/0277-3791(91)90033-Q

Bond G, Kromer B, Beer J, et al. 2001. Persistent solar influence on North Atlantic climate during the holocene. Science, 294(5549): 2130–2136, doi: 10.1126/science.1065680

Bond G, Showers W, Cheseby M, et al. 1997. A pervasive millennial-scale cycle in North Atlantic holocene and glacial climates. Science, 278(5341): 1257–1266, doi: 10.1126/science.278.5341.1257

Bradley S L, Milne G A, Horton B P, et al. 2016. Modelling sea level data from China and Malay-Thailand to estimate Holocene ice-volume equivalent sea level change. Quaternary Science Reviews, 137: 54–68, doi: 10.1016/j.quascirev.2016.02.002

Cai Yanjun, Cheng Xing, Ma Le, et al. 2021. Holocene variability of East Asian summer monsoon as viewed from the speleothem δ^{18}O records in central China. Earth and Planetary Science Letters, 558: 116758, doi: 10.1016/j.epsl.2021.116758

Chen J H, Edwards R L, Wasserburg G J. 1986. ^{238}U, ^{234}U and ^{232}Th in seawater. Earth and Planetary Science Letters, 80(3–4): 241–251, doi: 10.1016/0012-821X(86)90108-1

Chen Tianran, Li Shu, Zhao Jianxin, et al. 2021. Uranium-thorium dating of coral mortality and community shift in a highly disturbed inshore reef (Weizhou Island, northern South China Sea). Science of the Total Environment, 752: 141866, doi: 10.1016/j.scitotenv.2020.141866

Chen Yue-Gau, Liu Tsung-Kwei. 1996. Sea level changes in the last several thousand years, Penghu Islands, Taiwan Strait. Quaternary Research, 45(3): 254–262, doi: 10.1006/QRES.1996.0026

Cheng Lijing, Abraham J, Hausfather Z, et al. 2019. How fast are the oceans warming? Science, 363(6423): 128–129,doi: 10.1126/science.aav7619 doi: 10.1126/science.aav7619

China Nave Hydrographic Office. 2022. Guide to China Ports South China Sea. Tianjin: China Navigation Publications Press, 1–339

Claar D C, Szostek L, McDevitt-Irwin J M, et al. 2018. Global patterns and impacts of El Niño events on coral reefs: a meta-analysis. PLoS One, 13(2): e0190957, doi: 10.1371/journal.pone.0190957

Clark P U, Shakun J D, Baker P A, et al. 2012. Global climate evolution during the last deglaciation. Proceedings of the National Academy of Sciences of the United States of America, 109(19): E1134–E1142, doi: 10.1073/pnas.1116619109

Climate Change Center of the China Meteorological Administration. 2022. Blue Book on Climate Change in China 2022 (in Chinese). Beijing: Science Press, 1–109

Dalton S J, Carroll A G, Sampayo E, et al. 2020. Successive marine heatwaves cause disproportionate coral bleaching during a fast phase transition from El Niño to La Niña. Science of the Total Environment, 715: 136951, doi: 10.1016/j.scitotenv.2020.136951

Davis A M, Aitchison J C, Flood P G, et al. 2000. Late Holocene higher sea-level indicators from the South China coast. Marine Geology, 171(1–4): 1–5, doi: 10.1016/S0025-3227(00)00113-4

Dickinson W R. 2004. Impacts of eustasy and hydro-isostasy on the evolution and landforms of Pacific atolls. Palaeogeography, Palaeoclimatology, Palaeoecology, 213(3–4): 251–269, doi: 10.1016/j.palaeo.2004.07.012

Drinkwater K F, Beaugrand G, Kaeriyama M, et al. 2010. On the processes linking climate to ecosystem changes. Journal of Marine Systems, 79(3-4): 374–388, doi: 10.1016/j.jmarsys.2008.12.014

Dykoski C A, Edwards R L, Cheng Hai, et al. 2005. A high-resolution, absolute-dated Holocene and deglacial Asian monsoon record from Dongge Cave, China. Earth and Planetary Science Letters, 233(1-2): 71–86, doi: 10.1016/j.epsl.2005.01.036

Eisenhauer A, Wasserburg G J, Chen J H, et al. 1993. Holocene sea-level determination relative to the Australian continent: U/Th (TIMS) and ^{14}C (AMS) dating of coral cores from the Abrolhos Islands. Earth and Planetary Science Letters, 114(4): 529–547, doi: 10.1016/0012-821x(93)90081-j

Emanuel K. 2005. Increasing destructiveness of tropical cyclones over the past 30 years. Nature, 436(7051): 686–688, doi: 10.1038/nature03906

Engelhart S E, Horton B P, Kemp A C. 2011. Holocene sea-level changes along the United States' Atlantic coast. Oceanography, 24(2): 70–79, doi: 10.5670/oceanog.2011.28

Fallon S J, McCulloch M T, van Woesik R, et al. 1999. Corals at their latitudinal limits: laser ablation trace element systematics in *Porites* from Shirigai Bay, Japan. Earth and Planetary Science Letters, 172(3-4): 221–238, doi: 10.1016/S0012-821X(99)00200-9

Foster N L, Attrill M J. 2021. Chapter 20-Changes in coral reef ecosystems as an indication of climate and global change. In: Letcher T M, ed. Climate Change. 3rd ed. Amsterdam, The Netherlands: Elsevier, 427–443

Gagan M K, Ayliffe L K, Hopley D, et al. 1998. Temperature and surface-ocean water balance of the Mid-Holocene tropical Western Pacific. Science, 279(5353): 1014–1018, doi: 10.1126/science.279.5353.1014

Guan Yi, Hohn S, Merico A. 2015. Suitable environmental ranges for potential coral reef habitats in the tropical ocean. PLoS One, 10(6): e0128831, doi: 10.1371/journal.pone.0128831

Hall B L, Henderson G M. 2001. Use of uranium–thorium dating to determine past ^{14}C reservoir effects in lakes: examples from Antarctica. Earth and Planetary Science Letters, 193(3–4): 565–577, doi: 10.1016/s0012-821x(01)00524-6

Hallmann N, Camoin G, Eisenhauer A, et al. 2018. Ice volume and climate changes from a 6000 year sea-level record in French Polynesia. Nature Communications, 9(1): 285, doi: 10.1038/s41467-017-02695-7

Hamanaka N, Kan H, Yokoyama Y, et al. 2012. Disturbances with hiatuses in high-latitude coral reef growth during the Holocene: correlation with millennial-scale global climate change. Global and Planetary Change, 80–81: 21–35, doi: 10.1016/j.gloplacha.2011.10.004

Haug G H, Hughen K A, Sigman D M, et al. 2001. Southward migration of the intertropical convergence zone through the Holocene. Science, 293(5533): 1304–1308, doi: 10.1126/science.1059725

Hongo C, Kayanne H. 2010. Holocene sea-level record from corals: reliability of paleodepth indicators at Ishigaki Island, Ryukyu Islands, Japan. Palaeogeography, Palaeoclimatology, Palaeoecology, 287(1–4): 143–151, doi: 10.1016/j.palaeo.2010.01.033

Horton B P, Gibbard P L, Mine G M, et al. 2005. Holocene sea levels and palaeoenvironments, Malay-Thai Peninsula, southeast Asia. The Holocene, 15(8): 1199–1213, doi: 10.1191/0959683605hl891rp

Hua Quan, Ulm S, Yu Kefu, et al. 2020. Temporal variability in the Holocene marine radiocarbon reservoir effect for the Tropical and South Pacific. Quaternary Science Reviews, 249: 106613, doi: 10.1016/j.quascirev.2020.106613

Huang Deyin, Shi Qi, Zhang Yechun. 2007. Coral reef and high sea level at Luhuitou, Hainan Island during the Holocene. Marine Science Bulletin, 9(2): 61–70

Huang Zhenguo, Zhang Weiqiang, Chen Junhong. 1995. Plate tectonics and Quaternary volcanicity in China. Scientia Geographica Sinica (in Chinese), 15(2): 109–117

Hughes T P, Kerry J T, Álvarez-Noriega M, et al. 2017. Global warming and recurrent mass bleaching of corals. Nature, 543(7645): 373–377, doi: 10.1038/nature21707

Ingram B L, Southon J R. 1996. Reservoir ages in eastern pacific coastal and estuarine waters. Radiocarbon, 38(3): 573–582, doi: 10.1017/S0033822200030101

IPCC. 2021. Climate Change 2021: The Physical Science Basis. Contribution of Working Group I to the Sixth Assessment Report of the Intergovernmental Panel on Climate Change. Cambridge: Cambridge University Press

Klotzbach P J. 2006. Trends in global tropical cyclone activity over the past twenty years (1986–2005). Geophysical Research Letters, 33(10): L10805, doi: 10.1029/2006GL025881

Knutson T R, McBride J L, Chan J, et al. 2010. Tropical cyclones and climate change. Nature Geoscience, 3(3): 157–163, doi: 10.1038/ngeo779

Kriebel D L, Geiman J D, Henderson G R. 2015. Future flood frequency under sea-level rise scenarios. Journal of Coastal Research, 31(5): 1078–1083, doi: 10.2112/JCOASTRES-D-13-00190.1

Lambeck K, Rouby H, Purcell A, et al. 2014. Sea level and global ice volumes from the Last Glacial Maximum to the Holocene, Proceedings of the National Academy of Sciences, 111(43), 15296–15303, doi: 10.1073/pnas.1411762111

Landsea C W. 2005. Hurricanes and global warming. Nature, 438(7071): E11–E12, doi: 10.1038/nature04477

Liu Wenhui, Yu Kefu, Wang Rui, et al. 2020. Uranium-series ages of Beigang beachrock at Weizhou Island and their significance in recording sea level variations. Quaternary Sciences (in Chinese), 40(3): 764–774, doi: 10.11928/j.issn.1001-7410.2020.03.14

Lough J M. 2012. Small change, big difference: sea surface temperature distributions for tropical coral reef ecosystems, 1950–2011. Journal of Geophysical Research:Oceans, 117(C9): C09018, doi: 10.1029/2012jc008199

Lu Ruqi. 1997. Study on the modern crustal vertical movement in Guangdong coast. South China Journal of Seismology (in Chinese), 17(1): 25–33

Lu Bingquan, Wang Guozhong, Quan Songqing. 1984. The characteristics of fringing reefs of Hainan Island. Geographical Research (in Chinese), 3(3): 1–16

Ma Yifang, Qin Yeman, Yu Kefu, et al. 2021. Holocene coral reef development in Chenhang Island, Northern South China Sea, and its record of sea level changes. Marine Geology, 440: 106593, doi: 10.1016/j.margeo.2021.106593

Majewski J M, Switzer A D, Meltzner A J, et al. 2018. Holocene relative sea-level records from coral microatolls in Western Borneo, South China Sea. The Holocene, 28(9): 1431–1442, doi: 10.1177/0959683618777061

Meltzner A J, Switzer A D, Horton B P, et al. 2017. Half-metre sea-level fluctuations on centennial timescales from mid-Holocene corals of Southeast Asia. Nature Communications, 8: 14387, doi: 10.1038/ncomms14387

Meltzner A J, Woodroffe C D. 2015. Coral microatolls. In: Shennan I, Long A J, Horton B P, eds. Handbook of Sea - Level Research. Hoboken: Weley Blachwell, 125–145, doi: 10.1002/9781118452547.ch8

Montaggioni L F. 2005. History of Indo-Pacific coral reef systems since the last glaciation: development patterns and controlling factors. Earth-Science Reviews, 71(1-2): 1–75, doi: 10.1016/j.earscirev.2005.01.002

Morton B, Blackmore G. 2001. South China Sea. Marine Pollution Bulletin, 42(12): 1236–1263, doi: 10.1016/s0025-326x(01)00240-5

Moy C M, Seltzer G O, Rodbell D T, et al. 2002. Variability of El Niño/Southern Oscillation activity at millennial timescales during the Holocene epoch. Nature, 420(6912): 162–165, doi: 10.1038/nature01194

Nie Baofu. 1996. Sea-level changes of the South China Sea in the past 5000 years. Quaternary Sciences (in Chinese), 16(1): 80–87

Nunn P D. 2000. Significance of emerged Holocene corals around Ovalau and Moturiki islands, Fiji, southwest Pacific. Marine Geology, 163(1-4): 345–351, doi: 10.1016/S0025-3227(99)00114-0

Pan Huijuan, Chen Minte, Kong Deming, et al. 2020. Surface ocean hydrographic changes in the western Pacific marginal seas since the Early Holocene. Frontiers in Earth Science, 8: 200, doi: 10.3389/feart.2020.00200

Parham P R, Saito Y, Sapon N, et al. 2014. Evidence for ca. 7-ka maximum Holocene transgression on the Peninsular Malaysia east coast. Journal of Quaternary Science, 29(5): 414–422, doi: 10.1002/jqs.2714

Perry C T, Smithers S G. 2011. Cycles of coral reef 'turn-on', rapid growth and 'turn-off' over the past 8500 years: a context for understanding modern ecological states and trajectories. Global Change Biology, 17(1): 76–86, doi: 10.1111/j.1365-2486.2010.02181.x

Ramsay P J. 1996. 9000 Years of sea-level change along the southern

African coastline. Quaternary International, 31: 71–75, doi: 10.1016/1040-6182(95)00040-P
Rasmussen, S O, Andersen K K, Svensson A M, et al. 2006. A new Greenland ice core chronology for the last glacial termination, Journal of Geophysical Research, 111(D6), D06102, doi: 10.1029/2005JD006079
Romero–Torres T M, Acosta A, Palacio–castro A M, et al. 2020. Coral reef resilience to thermal stress in the eastern tropical pacific. Global Change Biology, 26(7): 3880–3890, doi: 10.1111/gcb.15126
Scoffin T P, Stoddart D R. 1978. The nature and significance of microatolls. Philosophical Transactions of the Royal Society B:Biological Sciences, 284(999): 99–122, doi: 10.1098/rstb.1978.0055
Shi Xiaojun, Yu Kefu, Chen Tegu, et al. 2008. Mid-to Late-Holocene sea level highstands: evidence from fringing coral reefs at Qionghai, Hainan Island. Marine Geology & Quaternary Geology (in Chinese), 28(5): 1–9
Sirocko F, Sarnthein M, Erlenkeuser H, et al. 1993. Century-scale events in monsoonal climate over the past 24, 000 years. Nature, 364(6435): 322–324, doi: 10.1038/364322a0
Smith D E, Harrison S, Firth C R, et al. 2011. The early Holocene sea level rise. Quaternary Science Reviews, 30(15-16): 1846–1860, doi: 10.1016/j.quascirev.2011.04.019
Smithers S. 2011. Microatoll. In: Hopley D, ed. Encyclopedia of Modern Coral Reefs: Structure, Form and Process. Dordrecht: Springer, doi: 10.1007/978-90-481-2639-2_111
Smithers S G, Woodroffe C D. 2000. Microatolls as sea-level indicators on a Mid-ocean atoll. Marine Geology, 168(1-4): 61–78, doi: 10.1016/S0025-3227(00)00043-8
Stattegger K, Tjallingii R, Saito Y, et al. 2013. Mid to late Holocene sea-level reconstruction of Southeast Vietnam using beachrock and beach-ridge deposits. Global and Planetary Change, 110: 214–222, doi: 10.1016/j.gloplacha.2013.08.014
Stirling C H, Esat T M, McCulloch M T, et al. 1995. High-precision U-series dating of corals from Western Australia and implications for the timing and duration of the Last Interglacial. Earth and Planetary Science Letters, 135(1-4): 115–130, doi: 10.1016/0012-821X(95)00152-3
Stoddart D R, Scoffin T P. 1979. Microatolls: review of form, origin and terminology. Atoll Research Bulletin, 224: 1–17, doi: 10.5479/si.00775630.224.1
Stott L, Cannariato K, Thunell R, et al. 2004. Decline of surface temperature and salinity in the western tropical Pacific Ocean in the Holocene epoch. Nature, 431(7004): 56–59, doi: 10.1038/nature02903
Taherkhani M, Vitousek S, Barnard P L, et al. 2020. Sea-level rise exponentially increases coastal flood frequency. Scientific Reports, 10(1): 6466, doi: 10.1038/s41598-020-62188-4
Tam C Y, Zong Yongqiang, bin Hassan K, et al. 2018. A below-the-present late Holocene relative sea level and the glacial isostatic adjustment during the Holocene in the Malay Peninsula. Quaternary Science Reviews, 201: 206–222, doi: 10.1016/j.quascirev.2018.10.009
Tanabe S, Hori K, Saito Y, et al. 2003. Song Hong (Red River) delta evolution related to millennium-scale Holocene sea-level changes. Quaternary Science Reviews, 22(21-22): 2345–2361, doi: 10.1016/S0277-3791(03)00138-0
Tang Lichao, Yue Yuanfu. 2023. Application and uncertainty analysis of beachrock to Mid-late Holocene sea-level reconstruction in the northern South China Sea. Marine Geology Frontiers (in Chinese), 39(3): 1–19, doi: 10.16028/j.1009-2722.2022.049
Tao Shichen, Yu Kefu, Yan Hongqiang, et al. 2022. Annual resolution records of sea-level change since 1850 CE reconstructed from coral δ18O from the South China Sea. Palaeogeography, Palaeoclimatology, Palaeoecology, 592(15): 110897, doi: 10.1016/j.palaeo.2022.110897
Vitousek S, Barnard P L, Fletcher C H, et al. 2017. Doubling of coastal flooding frequency within decades due to sea-level rise. Scientific Reports, 7(1): 1399, doi: 10.1038/s41598-017-01362-7
Wang Han-Sheng, Jia Lu-Lu, Wu P, et al. 2012. Long-Wei. Effects of last-deglaciation on the historical relative sea levels of East Asia Seas and the implications. Chinese Journal of Geophysics (in Chinese), 55(4): 1144–1153, doi: 10.6038/j.issn.0001-5733.2012.04.010
Wang Shaohong. 1989. Some problem on recognition of sea level indicators. Journal of Oceanography in Taiwan Strait (in Chinese), 8(4): 329–337
Wang Yongjin, Cheng Hai, Edwards R L, et al. 2005. The Holocene Asian monsoon: links to solar changes and North Atlantic climate. Science, 308(5723): 854–857, doi: 10.1126/science.1106296
Wang Shaowu, Gong Daoyi. 2000. Climate in China during the four special periods in Holocene. Progress in Natural Science (in Chinese), 10(4): 325–332
Wang Pingxian, Wang Bin, Cheng Hai, et al. 2017. The global monsoon across time scales: mechanisms and outstanding issues. Earth-Science Reviews, 174: 84–121, doi: 10.1016/j.earscirev.2017.07.006
Webster J M, Braga J C, Humblet M, et al. 2018. Response of the Great Barrier Reef to sea-level and environmental changes over the past 30, 000 years. Nature Geoscience, 11(6): 426–432, doi: 10.1038/s41561-018-0127-3
Webster J M, George N P J, Beaman R J, et al. 2016. Submarine landslides on the Great Barrier Reef shelf edge and upper slope: a mechanism for generating tsunamis on the north-east Australian coast? Marine Geology, 371: 120–129, doi: 10.1016/j.margeo.2015.11.008
Webster P J, Holland G J, Curry J A, et al. 2005. Changes in tropical cyclone number, duration, and intensity in a warming environment. Science, 309(5742): 1844–1846, doi: 10.1126/science.1116448
Wei Gangjian, Deng Wenfeng, Yu Kefu, et al. 2007. Sea surface temperature records in the northern South China Sea from mid-Holocene coral Sr/Ca ratios. Paleoceanography, 22(3): PA3206, doi: 10.1029/2006PA001270
Woodroffe C, McLean R. 1990. Microatolls and recent sea level change on coral atolls. Nature, 344(6266): 531–534, doi: 10.1038/344531a0
Wu Jing, Liu Q, Cui Qiaoyu, et al. 2019. Shrinkage of East Asia winter monsoon associated with increased ENSO events since the mid - holocene. Journal of Geophysical Research:Atmospheres, 124(7): 3839–3848, doi: 10.1029/2018jd030148
Xiong Haixian, Zong Yongqiang, Li Tanghua, et al. 2020. Coastal GIA processes revealed by the early to middle Holocene sea-level history of east China. Quaternary Science Reviews, 233: 106249, doi: 10.1016/j.quascirev.2020.106249
Xiong Haixian, Zong Yongqiang, Qian Peng, et al. 2018. Holocene sea-level history of the northern coast of South China Sea. Quaternary Science Reviews, 194: 12–26, doi: 10.1016/j.quascirev.2018.06.022
Yan Tingli, Yu Kefu, Wang Rui, et al. 2021. Records of sea-level highstand over the Meghalayan age/late Holocene from uranium-series ages of beachrock in Weizhou Island, northern South China Sea. The Holocene, 31(11-12): 1745–1760, doi: 10.1177/09596836211033215
Yan Shuang, Zhao Jianxin, Lau A Y A, et al. 2019. Episodic reef growth in the northern South China Sea linked to warm climate during the past 7, 000 years: potential for future coral refugia. Journal of Geophysical Research:Biogeosciences, 124(4): 1032–1043, doi: 10.1029/2018JG004939
Yang, Hongqiang, Yu Kefu, Zhao Meixia, et al. 2015. Impact on the coral reefs at Yongle Atoll, Xisha Islands, South China Sea from a strong typhoon direct sweep: Wutip, September 2013, Journal of Asian Earth Sciences 114, 457-466, doi: 10.1016/j.jseaes.2015.04.009
Yao Yantao, Zhan Wenhuan, Sun, Jinlong, et al. 2013. Emerged fossil corals on the coast of northwestern Hainan Island, China: implications for mid-Holocene sea level change and tectonic uplift. Chinese Science Bulletin, 58(23): 2869–2876, doi: 10.1007/s11434-013-5692-7
Yu Kefu. 2000. The sea surface temperature changing trend of the last

40 years in the Lei-Qiong sea area. Tropical Geography (in Chinese), 20(2): 111–115

Yu Kefu. 2012. Coral reefs in the South China Sea: their response to and records on past environmental changes. Science China Earth Sciences, 55(8): 1217–1229, doi: 10.1007/s11430-012-4449-5

Yu Kefu, Hua Quan, Zhao Jianxin, et al. 2010. Holocene marine ^{14}C reservoir age variability: evidence from ^{230}Th-dated corals in the South China Sea. Paleoceanography, 25(3): PA3205, doi: 10.1029/2009PA001831

Yu Kefu, Liu Dongshen, Shen Chengde, et al. 2002. High-frequency climatic oscillations recorded in a Holocene coral reef at Leizhou Peninsula, South China Sea. Science in China Series D:Earth Sciences, 45(12): 1057–1067, doi: 10.1360/02yd9103

Yu Kefu, Zhao Jinxin, Done T, et al. 2009. Microatoll record for large century-scale sea-level fluctuations in the Mid-Holocene. Quaternary Research, 71(3): 354–360, doi: 10.1016/j.yqres.2009.02.003

Yu Kefu, Zhao Jinxin, Liu Tung-Sheng, et al. 2004. High-frequency winter cooling and reef coral mortality during the Holocene climatic optimum, Earth and Planetary Science Letters, 224(1–2), 143–155, doi: 10.1016/j.epsl.2004.04.036

Yu Kefu, Zhao Jinxin, Shi Qi, et al. 2012. Recent massive coral mortality events in the South China Sea: was global warming and ENSO variability responsible? Chemical Geology, 320–321: 54–65, doi: 10.1016/j.chemgeo.2012.05.028

Yu Kefu, Zhao Jinxin, Wei Gangjian, et al. 2005. $\delta^{18}O$, Sr/Ca and Mg/Ca records of *Porites lutea* corals from Leizhou Peninsula, northern South China Sea, and their applicability as paleoclimatic indicators. Palaeogeography, Palaeoclimatology, Palaeoecology, 218(1–2): 57–73, doi: 10.1016/j.palaeo.2004.12.003

Yu Mugeng, Liu Jinfang. 1993. Current system and circulation feature of South China Sea. Marine Forecasts (in Chinese), 10(2): 13–17

Yue Yuanfu, Tang Lichao. 2023. Characteristics of sea level changes in the northern South China Sea since the Holocene and prediction of the future trends. Marine Geology Frontiers (in Chinese), 39(2): 1–16, doi: 10.16028/j.1009-2722.2022.193

Yue Yuanfu, Yu Kefu, Tao Shichen, et al. 2019. 3500-year western Pacific storm record warns of additional storm activity in a warming warm pool. Palaeogeography, Palaeoclimatology, Palaeoecology, 521: 57–71, doi: 10.1016/j.palaeo.2019.02.009

Yue Yuanfu, Zheng Zhuo, Huang Kangyou, et al. 2012. A continuous record of vegetation and climate change over the past 50, 000years in the Fujian Province of eastern subtropical China. Palaeogeography, Palaeoclimatology, Palaeoecology, 365–366: 115–123, doi: 10.1016/j.palaeo.2012.09.018

Zhan Wenhuan, Zhang Zhiqiang, Sun Jie, et al. 2007. Analysis of crustal fluctuation rate in the northwestern South China Sea coral reef area (in Chinese). In: Proceedings of the 23rd Annual Meeting of Chinese Geophysical Society. Qingdao: China Ocean University Press, 720

Zhang Keqi, Douglas B C, Leatherman S P. 2004. Global warming and coastal erosion. Climatic Change, 64(1): 41–58, doi: 10.1023/B:CLIM.0000024690.32682.48

Zhang Zhenke, Meng Hongming, Wang Wanfang, et al. 2008. Preliminary study on the coastal sediments records about the historical earthquake in the year of 1605, Hainan Island, China. Marine Geology & Quaternary Geology (in Chinese), 28(3): 9–14

Zhang Yuanzhi, Xie Jizhen, Liu Llin. 2011. Investigating sea-level change and its impact on Hong Kong's coastal environment. Annals of GIS, 17(2): 105–112, doi: 10.1080/19475683.2011.576268

Zhang Yaze, Zong Yongqiang, Xiong Haixian, et al. 2021. The middle-to-late Holocene relative sea-level history, highstand and levering effect on the east coast of Malay Peninsula. Global and Planetary Change, 196: 103369, doi: 10.1016/j.gloplacha.2020.103369

Zhao Xitao. 1983. Development of Holocene coral reefs in China and their reflection on sea level changes and tectonic movement. Science in China Series B-Chemistry, Biological, Agricultural, Medical & Earth Sciences, 26(4): 413–423, doi: 10.1360/yb1983-26-4-413

Zhao Jinxin, Yu Kefu. 2002. Timing of Holocene sea-level highstands by mass spectrometric U-series ages of a coral reef from Leizhou Peninsula, South China Sea. Chinese Science Bulletin, 47(4): 348–352, doi: 10.1007/BF02901194

Zong Yongqiang. 2004. Mid-Holocene sea-level highstand along the Southeast Coast of China. Quaternary International, 117(1): 55–67, doi: 10.1016/S1040-6182(03)00116-2

Zong Yongqiang, Huang Kuangyou, Yu Fengling, et al. 2012. The role of sea-level rise, monsoonal discharge and the palaeo-landscape in the early Holocene evolution of the Pearl River delta, southern China. Quaternary Science Reviews, 54: 77–88, doi: 10.1016/j.quascirev.2012.01.002

Supplementary information:

Fig. S1. Mean monthly temperature, precipitation, humidity and wind speed of Qionghai, Hainan Island (data from Qionghai Meteorological Station during 1980–2010 CE).

Table S1. Multi-year mean monthly data of Qionghai meteorological station from 1980 to 2010, Hainan Island.

Table S2. Surface elevation (relative to modern MSL) of the 27 live Porites from Tongguling along the coast of Wenchang, Hainan Island in the northern SCS.

Table S3. U-Th isotopic data, age, relative elevation, elevation of tectonic uplift and indicated paleao-sea-level elevation derived from our 3 new in-situ Porites and previous 19 in situ Porites from the eastern coast of Hainan Island in the northern SCS.

Table S4. U-Th dating data of in-situ corals from the northern SCS which provided much information on the episodes of coral growth. All the ages were converted into calendar years before present (cal a BP, where “present” is relative to 1950 CE), and were presented in cal a BP in this study. All U-Th data errors are 2σ standard deviation.

The supplementary information is available online at https:/doi.org/10.1007/s13131-023-2264-9 and http://www.aosocean.com/. The supplementary information is published as submitted, without typesetting or editing. The responsibility for scientific accuracy and content remains entirely with the authors.